Modeling of reflected and scattered light intensity of ordered mesoporous layers of silica

Pierre Cheyssac, A.Ten Bosch

Modeling of reflected and scattered light intensity of ordered mesoporous layers of silica

P. Cheyssac *, A. ten Bosch

Laboratoire de Physique de la Matière Condensée, UMR 6622 CNRS, Université de Nice-Sophia Antipolis, Faculté des Sciences, Parc Valrose, 06108 Nice Cedex 2, France

Abstract

Mesoporous materials are characterized by the density of empty or filled pores which modulates their properties, in particular, optical properties. Although pores scatter light, the scattered energy or reflectance spectra of a mesoporous layer show a behaviour that can be attributed mainly to interference created by the interfaces; however, coherent scattering is still present inside the mesoporous layer. In this paper, we show that diffusively reflected light created by the pores depends on their distribution and shape. If they are distributed along a periodic lattice, the structure factor modulates the optical properties and the form factor that describes the geometry of the pores, influences the shape of optical spectrum. We study the influence of the form factor of pores which renders possible a tuning of the optical reflectance spectrum through pore geometry.

Keywords: Mesoporous materials; Geometry of pores; Scattering properties

1. Introduction

Mesoporous materials are artificial materials with potential optical applications [1]. They contain pores, that may be filled or not, dispersed in an amorphous dielectric matrix. Properties such as their dielectric constant [2,3] are tunable by varying the filling factor or pore density [4].

Reflectance, spectroscopic ellipsometry, diffuse transmission spectrocopies [5] and angularly resolved transmission of diffusive materials have been reported [6]. The angular distribution of light back scattered by a mesoporous film [7] shows an interference pattern in contrast to [5,6]. The specular reflection spectrum $R_{\mathrm{exp}}(\lambda)$, of a mesoporous silica film deposited on a silicon oxide film on top of a Si wafer, has also been measured [8] close to normal incidence from $\lambda = 400$ to 800 nm. It exhibits characteristic interference fringes. A Fresnel description that combines the effects of the interfaces, thickness of layers and indices of the sample, can explain the specular $R_{\mathrm{exp}}(\lambda)$ reflectance spectrum, as will be recalled briefly below.

We will show that diffusively reflected spectra may also exhibit an interference pattern that does not originate from interfaces but from the internal structure of the mesoporous layer.

2. Fresnel reflectance

We consider a mesoporous silica film of thickness d_2=490.2 nm [8] deposited on a SiO_2+Si substrate; the relevant synthesis and structure have already been given in detail in [9, 10]. Pores are ordered in a unidirectional compressed close packed hexagonal structure; assuming a spherical shape, their size ϕ was estimated as 3.6 nm [11,12] and the filling factor q reaches values as high as 0.43.

From a theoretical point of view, and neglecting scattering, the Fresnel reflectance $R_{\mathrm{Fresnel}}(\lambda, q)$ of this multi-layered sample has been described, provided reflection comes from the interfaces alone, by a combination of the various thicknesses and indices. We define the reflectance coefficients ρ_{ij} with ρ_{12} for the vacuum–mesoporous layer, ρ_{23} for mesoporous layer-SiO_2 and ρ_{34} for SiO_2–Si interfaces respectively. Then, let us write

$$\rho_{24} = \frac{\rho_{23} + \rho_{34} e^{2ik_3 d_3}}{1 + \rho_{23}\rho_{34} e^{2ik_3 d_3}} \tag{1}$$

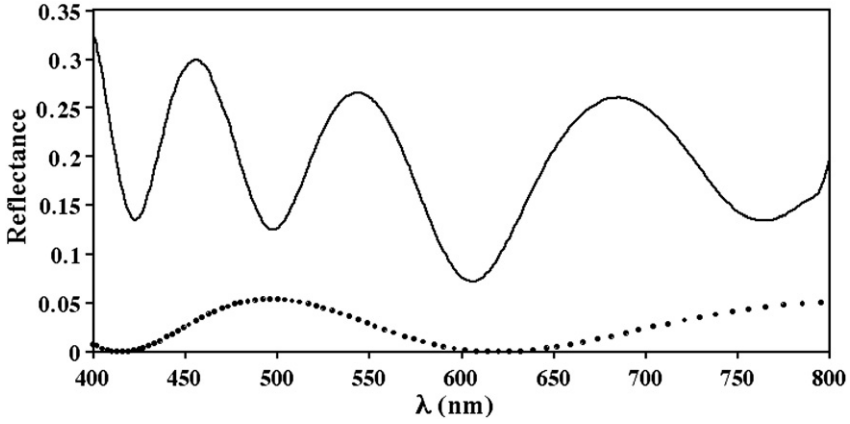

Fig. 1. Reflectance spectrum $R_{\text{Fresnel}}(\lambda, q)$ of a supported mesoporous film: experiment- continuous line, and calculated $R'_{\text{Fresnel}}(\lambda, q)$ Fresnel reflectance of the same non-supported mesoporous film- dotted line.

where k_i is the wave vector and d_i the thickness of the ith layer. $R_{\text{Fresnel}}(\lambda, q)$ of the multi-layered film is

$$R_{\text{Fresnel}}(\lambda, q) = \rho\ \rho^* = \left[\frac{\rho_{12} + \rho_{24}e^{2ik_2d_2}}{1 + \rho_{12}\rho_{24}e^{2ik_2d_2}}\right]\left[\frac{\rho_{12} + \rho_{24}e^{2ik_2d_2}}{1 + \rho_{12}\rho_{24}e^{2ik_2d_2}}\right]^* \quad (2)$$

The observed interference spectrum of the multi-layered film results from the Fresnel relations, i.e. a coherent combination of indices and plane waves reflected by interfaces: and good agreement between experimental and calculated Fresnel reflectance $R_{\text{Fresnel}}(\lambda, q)$ has been achieved [13].

The optical spectrum of this multi-layered sample depends strongly on the properties of the underlying SiO_2+Si substrate; therefore, it is not representative of the intrinsic properties of the mesoporous layer alone. In the case of a free-standing mesoporous layer with the same thickness d_2, ρ_{24} simplifies: $\rho_{24}=\rho_{23}$ and, neglecting scattering, its reflectance $R'_{\text{Fresnel}}(\lambda, q)$ is

$$R'_{\text{Fresnel}}(\lambda, q) = \rho\ \rho^* = \left[\frac{\rho_{12} + \rho_{23}e^{2ik_2d_2}}{1 + \rho_{12}\rho_{23}e^{2ik_2d_2}}\right]\left[\frac{\rho_{12} + \rho_{23}e^{2ik_2d_2}}{1 + \rho_{12}\rho_{23}e^{2ik_2d_2}}\right]^* \quad (3)$$

Fig. 1 gives respectively the experimental $R_{\text{Fresnel}}(\lambda, q)$ for the supported and the calculated $R'_{\text{Fresnel}}(\lambda, q)$ spectra for the non-supported mesoporous films. At normal incidence, the intensity reflected by a free-standing mesoporous film contains Fresnel reflectance as well as back-scattered light.

Experimental results obtained on a free-standing mesoporous film could provide a possibility to distinguish between light reflected by interfaces and coherent scattering due to the internal structure of the mesoporous layer. The effect of diffusive back-scattering by a sample illuminated at normal incidence is now considered.

3. Diffusive scattering

The crystallographic structure of N pores within the sample is characterised by a periodic lattice. In light scattering, the corresponding structure factor defines a global behaviour of scattering. Pore centers are located at lattice sites $\overrightarrow{R_n} = n_1c_1\overrightarrow{e_x} + n_2c_2\overrightarrow{e_y} + n_3c_3\overrightarrow{e_z}$. The pore geometry, shape and orientation, are characterised by a form factor. As a consequence, the global behaviour already determined by the structure factor is modulated by the form factor.

What follows intends to show that it is possible to link the geometry of pores in a mesoporous film to the optical spectra created by the internal scattering. For example, in reflectance and scattering measurements performed at normal incidence, $\overrightarrow{k}$ is the wave vector of the incoming plane wave, $\overrightarrow{k'}$ the scattering wave vector, and both are along the z-axis and $k = |\overrightarrow{k'}|$. The scattered wave vector is $\overrightarrow{k_s} = \overrightarrow{k'} - \overrightarrow{k}$.

The incoming plane wave at $\overrightarrow{r_n}$ is $\overrightarrow{E} = \overrightarrow{E_0}e^{i\overrightarrow{k}\overrightarrow{r_n}}$. In the far field regime, the scattering amplitude due to the pore at $\overrightarrow{r_n}$ is $f(\overrightarrow{k}, \overrightarrow{k'}) = -\int\frac{dV}{4\pi}e^{-i\overrightarrow{k'}\overrightarrow{r_n}}\left[\overrightarrow{k}\times\overrightarrow{k'}\times(\overrightarrow{e_r}-1)\overrightarrow{E}(\overrightarrow{k}, \overrightarrow{r_n})\right]$; the scattered wave at distance R is $\overrightarrow{E_s} = f(\overrightarrow{k}, \overrightarrow{k'})\frac{e^{ikR}}{R}$ and $kR \gg 1$.

The dielectric tensor of the pore interior is ε and ε_m that of the matrix; then, $\varepsilon_r = \frac{\varepsilon}{\varepsilon_m}$ is the average relative dielectric

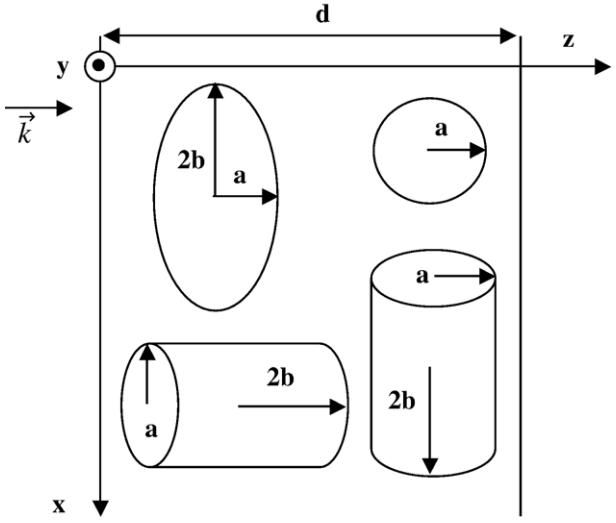

Fig. 2. Description of the geometries used.

constant. In the Rayleigh–Gans approximation [14], the electric far field scattered by a transparent inclusion in another transparent medium is calculated [15]. The distribution of scattered light is defined by the differential cross-section

$$\frac{d\sigma}{d\Omega} = \left|\frac{E_s}{E_0}\right|^2 R^2 \tag{4}$$

Pores may exhibit various geometries such as spheres or cylinders of different orientation in the film, associated with different form factors but the same structure factor. More explicitly in terms of these factors:

$$\frac{d\sigma}{d\Omega} = \frac{k^4}{4\pi^2}(\varepsilon_r - 1)^2 u^2(k_s) S(k_s) N. \tag{5}$$

The position $\vec{r_n}$ within the pore n (n=1 to N), is measured by $\vec{r}$ relative to the center of the pore $\vec{R_n}$ and $\vec{r_n} = \vec{r} + \vec{R_n}$. The structure factor is $S(\vec{k_s}) = \frac{1}{N}\sum_{n\neq n'} e^{i\vec{k_s}(\vec{Rn} - \vec{Rn'})}$. The form factor of the individual objects of volume V is defined as $u(\vec{k_s}) = |\int_v e^{-i\vec{k_s}\,\vec{r}}\,dV|$.

Differential scattered intensities for fixed scattered wave vector $\vec{k_s}$ or wavelength have been calculated for various form factors. Here, the direction of propagation of the incoming wave is along z-axis; and the corresponding model structure factor is $S(k_s) = \frac{1-\cos(d\ k_s)}{1-\cos(c\ k_s)} N_p$, where N_p is the number of pores for a given area of experiment. The width d or experimental thickness of the mesoporous layer involves the mean spacing c between pores. Fig. 2 describes the various geometries that are studied below.

For spherical pores [11,12] of radius a, the form factor $u_1(\vec{k_s})$ is calculated as

$$u_1^2(\vec{k_s}) = \frac{16\pi^2}{k_s^6}[\sin(k_s a) - k_s a\cos(k_s a)]^2. \tag{6}$$

For small pores, $k_s a \ll 1$, and $u_1^2(k_s) = \frac{16\pi^2 a^6}{9}$ is independent of k_s.

For ellipsoidal pores, 2b being the long axis and a the short one, the form factor is

$$u_2^2(k_2) = \frac{16\pi^2 b^4}{k_s^2 (k_s a)^4}[\sin(k_s a) - k_s a\cos(k_s a)]^2. \tag{7}$$

We have also considered finite cylinders, 2b being their long axis and a the radius. If cylinders are horizontal, i.e. parallel to the z-axis, 2b is along z and the form factor is

$$u_3^2(k_s) = \frac{2\pi^2 a^4}{k_s^2}[1 - \cos(2k_s b)] \tag{8}$$

If they are vertical, i.e. perpendicular to the z-axis, 2b is in the x–y plane, J_1 is the Bessel function and the form factor is [16]

$$u_4^2(\vec{k_s}) = \frac{16\pi^2 b^2 a^2}{k_s^2} J_1^2(ak_s). \tag{9}$$

Differential cross-sections of spheres and ellipsoids are given in Fig. 3 while Fig. 4 gives the results for horizontal and vertical cylinders. Geometrical parameters defining pores have been chosen close to the radius of the spherical pores quoted in [11,12]; other parameters are adjusted in order to fit, as far as possible, the best least square deviation between position and shape of calculated and experimental extrema available for the supported mesoporous film. The scattering cross-section (3) is related to the collected experimental power of scattered light through a numerical factor F containing the number of pores seen in the experiment [17] with $\frac{d\sigma}{d\Omega}F$ = ratio of scattered to incident power.

Cylinders perpendicular to z-axis, give the closest calculated shape and positions of extrema to the experimental results, the curve has been fit using F=200 nm^{-2}; this numerical value is discussed below.

4. Discussion

It has been briefly demonstrated that, in the case of a supported mesoporous layer, the measured intensity is mainly

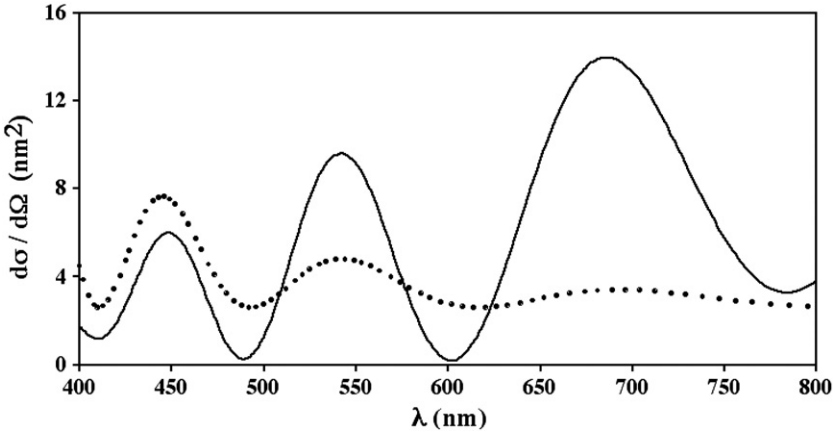

Fig. 3. Differential cross-sections of scattering for spherical:— continuous line, and ellipsoidal pores:— dotted line; sphere radius: =3.6 nm and mean spacing c=8 nm ellipsoid: long axis=3.6 nm, short axis=3.4 nm and mean spacing c=6.9 nm.

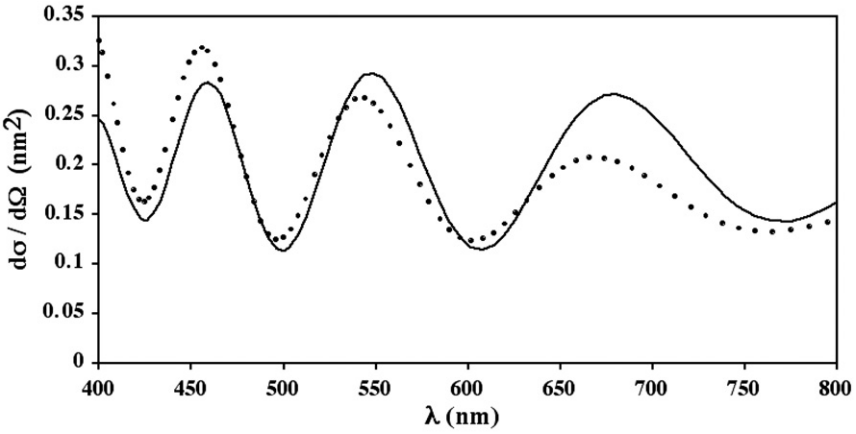

Fig. 4. Differential cross-sections of scattering for cylinders: horizontal cylinders: 2b=5.5 nm, radius 2.95 nm and mean spacing c=7.2 nm,– continuous line; vertical cylinders: height=5.5 nm, radius 3.56 nm and mean spacing c=6.94 nm,– dotted line.

the result of Fresnel reflectance. The good agreement obtained between calculated and experimental $R_{\mathrm{Fresnel}}(\lambda, q)$ spectra of the supported mesoporous [13] film shows that the influence of scattered intensity in the specular direction remains small and provides reasonable confidence in the calculated $R_{\mathrm{Fresnel}}'(\lambda, q)$ spectrum of a free-standing mesoporous film. Fig. 1 shows that the reflectance of a free-standing film is smaller than the supported one by a factor 5 to 6.

Since $|\varepsilon_r - 1| \ll 1$ and $kb|\varepsilon_r - 1| \ll 1$, the Rayleigh–Gans approximation for scattering by the mesopores is valid. The light beam propagates in z-direction; in the x–y plane, the mesoporous domains are small compared to that of the beam. Then, the measured spectra of the mesoporous layer along z-axis is an average between all orientations of pores in the x–y plane. However, long and short dimensions have been oriented along x and y axes in order to simplify the form factors in the various pore geometries.

Multiple scattering exists; its effect has been taken into account by including two scattering vectors k_{s1} and k_{s2} in the numerical simulations. Three or more scattering vectors do not change the general behaviour of the simulated differential cross-sections, and no significant decrease of the standard deviation between simulated and experimental spectra occurs. The mean values of k_{s1} and k_{s2} are respectively $9.8k$ and $11.9k$. In previous papers [11,12], pores were assumed to be spherical of mean diameter estimated as 3.6 nm. Although pores may deviate from spherical shape, the geometrical dimensions involved in form factors should remain the order of this estimated value.

As expected, the results are sensitive to the form factor. The main criteria for determining the best geometry of pores are the decreasing or increasing behaviour of $\frac{\mathrm{d}\sigma}{\mathrm{d}\Omega}$ with λ and the ratio of peak amplitudes and the best fit to experimental reflectance was found for cylinders perpendicular to the z-axis (see Fig. 4). The parameters a and b were fixed by a=2.953 nm and b=5.5 nm; these values are the order of the published pore size.

Because of the lack of experimental Fresnel reflectance or angular distribution of intensity scattered by a free-standing film, the simulation was applied to a supported film and resulted in a high F=200 nm^{-2}. The value of this factor is expected to be lower. For $F \approx 30$ nm^{-2} the scattering calculated from Eqs. (5) and (9) is of the same order of magnitude as the calculated reflectance of Eq. (3). Actually, a measured spectrum contains both Fresnel reflectance and scattered light even at normal incidence and any difference between the calculated Fresnel and measured spectra is evidence of the influence of scattering created by the mesoporous structure.

5. Conclusion

In this paper, we have studied the reflectance spectra created by supported and free-standing mesoporous layers. We have briefly recalled that, in both cases, interferences are due to interfaces. However, scattered light is present and its distribution is interpreted, in the framework of Rayleigh–Gans theory, as created by an ensemble of pores distributed in a crystal lattice. The lattice has been characterized by its structure factor and spherical, ellipsoidal and cylindrical pores by their form factors. The simulations show that different form factors lead to notable changes in the calculated spectra. For our supported mesoporous layer, it has been possible to identify that scattering by cylinders perpendicular to z-axis is in good agreement with experimental spectra, although the intensity due to scattering appears too small to explain the experiments, which are dominated by Fresnel interference. This is not true for angular measurements where scattering is predominant.

References

[1] J. Wang, G.D. Stucky, Adv. Funct. Mater. 14 (2004) 409.
[2] H. Fan, H.R. Bentley, K.R. Kathan, P. Clem, Y. Lu, C.J. Brinker, J. Non-Cryst. Solids 285 (2001) 79.
[3] C.-M. Yang, A.-T. Cho, F.-M. Pan, T.-G. Tsai, K.-J. Chao, Adv. Mater. 13 (2001) 1099.
[4] F.K. de Theije, A.R. Balkenende, M.A. Verheijen, M.R. Baklanov, K.P. Mogilnikov, Y. Furukawa, J. Phys. Chem., B. 107 (2003) 4280.
[5] M.U. Veran, D.J. Durian, Phys. Rev., E 53 (1996) 3215.
[6] J. Gomez Rivas, D.H. Dau, A. Imhof, R. Sprika, B.P.J. Bret, P.M. Johnson, T.W. Hijmans, A. Lagendijk, Opt. Commun. 220 (2003) 17.
[7] P. Cheyssac, M. Klotz, E. Søndergård, V.A. Sterligov, Opt. Commun. 252 (2005) 344.

[8] P. Cheyssac, M. Klotz, E. Søndergård, Thin Solid Films 495 (2006) 237.
[9] M. Klotz, A. Ayral, C. Guizard, L. Cot, J. Mater. Chem. 10 (2000) 663.
[10] M. Klotz, P.-A. Albouy, A. Ayral, C. Ménager, D. Grosso, A. Van der Lee, V. Cabuil, F. Babonneau, C. Guizard, Chem. Mater. 12 (2000) 1721.
[11] M. Klotz, S. Besson, C. Ricolleau, F. Bosc, A. Ayral, Membranes-Preparation, Properties and Applications, Boston, USA, 2–6 december 2002, in: V.N. Burganos, R.D. Noble, M. Asaeda, A. Ayral, J.D. LeRoux (Eds.), Mater. Res. Soc. Symp. Proc., 752, 2002, p. 123.
[12] S. Besson, T. Gacoin, C. Ricolleau, C. Jacquiod, J.-P. Boilot, Nano Lett. 2 (2002) 409.
[13] P. Cheyssac, Opt. Commun. 268 (2006) 273.
[14] R. Gans, Ann. Phys. 76 (1925) 29.
[15] S. Zumer, J.W. Doane, Phys. Rev., A. 34 (1986) 3373.
[16] C.F. Bohren, D.R. Hoffman, Absorption and Scattering of Light by Small Particles, John Wiley and Sons, New-York, 2004.
[17] H. Gratz, A. Penzkofer, P. Weidner, J. Non-Cryst. Solids 189 (1995) 50.